Modulation of synaptic potentials and cell excitability by dendritic K_{IR} and K_{As} channels in nucleus accumbens medium spiny neurons: A computational study

JESSY JOHN* and ROHIT MANCHANDA

Biomedical Engineering group, Department of Biosciences and Bioengineering, Indian Institute of Technology Bombay, Powai, Mumbai 400 076, India

**Corresponding author (Fax, +91-2225764770, +91-2225723480; Email, jessyroy@iitb.ac.in, jessyjohnroy@gmail.com)*

The nucleus accumbens (NAc), a critical structure of the brain reward circuit, is implicated in normal goal-directed behaviour and learning as well as pathological conditions like schizophrenia and addiction. Its major cellular substrates, the medium spiny (MS) neurons, possess a wide variety of dendritic active conductances that may modulate the excitatory post synaptic potentials (EPSPs) and cell excitability. We examine this issue using a biophysically detailed 189-compartment stylized model of the NAc MS neuron, incorporating all the known active conductances. We find that, of all the active channels, inward rectifying K^+ (K_{IR}) channels play the primary role in modulating the resting membrane potential (RMP) and EPSPs in the down-state of the neuron. Reduction in the conductance of K_{IR} channels evokes facilitatory effects on EPSPs accompanied by rises in local input resistance and membrane time constant. At depolarized membrane potentials closer to up-state levels, the slowly inactivating A-type potassium channel (K_{As}) conductance also plays a strong role in determining synaptic potential parameters and cell excitability. We discuss the implications of our results for the regulation of accumbal MS neuron biophysics and synaptic integration by intrinsic factors and extrinsic agents such as dopamine.

[John J and Manchanda R 2011 Modulation of synaptic potentials and cell excitability by dendritic K_{IR} and K_{As} channels in nucleus accumbens medium spiny neurons: A computational study. *J. Biosci.* **36** 309–328] **DOI** 10.1007/s12038-011-9039-8

1. Introduction

The nucleus accumbens (NAc), which predominantly constitutes the ventral striatum, acts as an interface between the limbic and extrapyramidal motor systems (Mogenson *et al.* 1980; Meredith and Totterdell 1999; Cooper 2002). It integrates motivational inputs related to emotional salience and contextual constraints from limbic structures such as ventral hippocampus and basolateral amygdale, on the one hand, and executive/motor inputs from medial prefrontal cortex, on the other (Mogenson 1987; Goto and O'Donnell 2002; Goto and Grace 2008). These glutamatergic inputs are modulated by dopaminergic inputs from ventral tegmental area (Yang and Mogenson 1984; Goto and Grace 2005a, b) that signal the reward stimuli (Kalivas and Nakamura 1999; Schultz 1998; Brady and O'Donnell 2004; Nicola *et al.* 2004). The integrated output is sent back to the cortex via ventral pallidum and medial thalamus (O'Donnell and Grace 1995) in order to generate appropriate responses in goal-directed behaviour. In addition to the normal goal-directed behaviour, the NAc is also believed to be involved in pathological conditions such as schizophrenia and drug

Keywords. Computational model; excitatory post synaptic potential (EPSP); inward rectifying K^+ (K_{IR}) channel; medium spiny neurons; nucleus accumbens slowly inactivating A-type potassium channel (K_{As}); spiking

Abbreviations used: AMPA, alpha-amino-3-hydroxy-5-methyl-4-isoxazole propionic acid; DA, dopamine; D1R, D1 receptor; D2R, D2 receptor; EPSPs, excitatory post synaptic potentials; GABA, gamma amino butyric acid; ISI, interspike interval; K_{IR}, inward rectifying potassium; MS, medium spiny; NAc, nucleus accumbens; NMDA, *N*-methyl-D-aspartate; RMP, resting membrane potential; K_{As}, slowly inactivating A-type potassium

addiction, where the normal brain reward circuit is distorted (O'Donnell and Grace 1998; Grace 2000; Cooper 2002; Wolf 2002; Carlezon and Thomas 2009).

The inputs to the NAc are integrated at the level of single neurons, the medium spiny (MS) neurons, which constitute the primary neurons of the NAc (O'Donnell and Grace 1995; French and Totterdell 2002; French and Totterdell 2003; McGinty and Grace 2009) and respond to the changes in reward-related behaviour and learning (Schultz *et al.* 2003; Carelli 2004). Studies using *in vitro* slices and *in vivo* anesthetized preparations have shown that these neurons display a two-state behaviour of the membrane potential in which the neurons remain preferentially in either a hyperpolarized down-state (~ −86 mV) or a depolarized up-state (~ −55 mV), depending on its inputs (O'Donnell and Grace 1993, 1995) as well as the presence of ionic currents (Nisenbaum and Wilson 1995; Wilson and Kawaguchi 1996; Cooper and White 2000; Nicola *et al.* 2000, 2004). Majority of the dopaminergic inputs to the MS neurons are located at the dendritic shafts and spines that also receive extensive glutamatergic excitatory inputs from the cortex or hippocampus (Smith and Bolam 1990; Meredith *et al.* 2008). The close proximity of these inputs has been suggested as a cellular mechanism that mediates reward-related learning in striatum (Reynolds *et al*. 2001).

In central neurons, dendritic active conductances are known to influence the input–output properties of the neuron including synaptic integration, neuronal excitability and synaptic plasticity (Magee *et al.* 1998). When activated, the currents through these channels can alter the amplitude and time course of the synaptic potentials (Reyes 2001). Moreover, voltage-gated channels alter the local input resistance and membrane time constant, which in turn influence both spatial and temporal summation of EPSPs (Johnston *et al.* 1996). For example, the hyperpolarization-activated cation (I_h) currents present in the dendrites of neocortical L5 and hippocampal pyramidal neurons act to reduce the overall neuronal excitability. I_h channels, being partially activated at rest, contribute to the resting potential of these cells and reduce their input resistance (Reyes 2001), resulting in EPSPs of smaller amplitude and faster decay (shorter duration) (Magee 1998; Williams and Stuart 2000; Migliore and Shepherd 2002; Biel *et al*. 2009). An active channel with an I-V curve bearing a resemblance to that of the I_h channel is also present in NAc MS neurons (the K_{IR} channel), in addition to a wide variety of other active channels that might potentially influence their input–output behaviour. These channels include voltage-dependent fast and persistent Na^+ channels (NaF and NaP), fast and slow A-type K^+ channels (K_{AF} and K_{AS}), and different types of Ca^{2+} (CaN, CaQ, CaR, CaT and L- type $Ca_v1.2$ and $Ca_v1.3$) as well as the small- and large-conductance Ca^{2+}-dependent K^+ channels (SKK_{Ca} and BKK_{Ca}) (Wolf *et al.* 2005). It is believed that the intrinsic properties of these neurons can be modulated and, thereby, neuronal excitability, by extrinsic factors such as dopamine that forms a major neuromodulator in the NAc (Nicola *et al*. 2000).

While some information is available about the conductances instrumental in maintaining the up- and down-states of the neuron (Wolf *et al*. 2001; Nicola *et al*. 2004), experimental studies on the roles of this wide array of active channels on EPSP propagation and synaptic integration have not been carried out in NAc MS neurons. Computational models provide a useful means of formulating experimentally testable predictions about the input–output behaviour of the neuron. Investigations on the role of K_{IR} channels in determining the membrane electrical properties in neostriatal neurons have been carried out in a previous computational work (Wilson 1992, 1993) that used a reduced model of the neuron with just two conductances – the K_{IR} and leak conductances. These studies indicated that K_{IR} plays a dominant role in modulating the electrical behaviour of the neuron in the down-state. However, as indicated earlier, as recent studies have shown that striatal neurons possess a wide range of nonlinear active channels and a biophysically more detailed model of the neuron incorporating all these channels is currently available in the literature (Wolf *et al*. 2005, Steephen and Manchanda 2009), we wished to investigate in detail (i) whether K_{IR} conductance continues to play a dominant role in the down-state even in the presence of the other non-linear active conductances in the neuron and (ii) whether any of the other channels plays a role in modulating the EPSPs in NAc MS neurons in the down-state as well as in the depolarized membrane potentials of the neuron. We find that, in the down-state, while the contribution from most channels is absent or negligibly small, dendritic K_{IR} channels do contribute significantly to this modulation even in the presence of other active conductances. However, at depolarized membrane potentials brought about by the blocking of K_{IR} conductance, K_{As} channels secondarily modulate the somatic EPSPs. As it is expected that at increasingly depolarized potentials the K_{As} conductance would play a progressively significant role compared with K_{IR}, we have also delineated the influence of K_{As} on EPSPs at relatively depolarized membrane potentials and also on the spiking behaviour of the neuron during the up-state.

A further motivation for exploring the effects of the K_{IR} conductance on MS neuron biophysics stems from the reports that this conductance is a major target of modulation by neurotransmitters such as dopamine, the direction of modulation being dependent on the type of dopamine receptors present in these neurons. Therefore, we investigated the effects of varying the conductance of K_{IR} channels on down-state EPSPs and the possible mechanisms underlying these effects. We find that reduction in K_{IR} conductance results in depolarization of the RMP and enhancement of the amplitude and temporal indices of the EPSP.

Analogous to the results reported by Wilson (1992), we find that these effects are accompanied by the changes in electrical properties of the cell membrane that appear to be responsible for the observed effects. The similarities in the I-V curves of K_{IR} channels in MS neurons and I_h channels in pyramidal neurons prompted us to the conjecture that the some of the effects due to I_h channels on pyramidal neuron biophysics, such as normalization of synaptic potentials at the soma, might be mirrored in MS neurons through K_{IR} channels. We find that K_{IR} conductance contribute to the normalization of synaptic potentials in NAc MS neurons. We discuss our findings in relation to MS neuron membrane biophysics as well as the neuron functioning with respect to synaptic input processing. Portions of this work have appeared in abstract form (John and Manchanda 2009).

2. Methods

In this study, data from published models (Wolf *et al.* 2005; Steephen and Manchanda 2009) were used to build a 189-compartment stylized model of the NAc MS neuron using the NEURON simulation platform (Carnevale and Hines 2006). The radially symmetric model included a soma and 4 proximal dendrites, each of which bifurcate twice to form 8 middle dendrites and 16 distal dendrites (figure 1A). Spatial discretization using the d-lambda rule (d-lambda value=0.15) resulted in a single compartment for the soma and each of the proximal and middle dendrites and 11 compartments for the long distal dendrites (figure 1B). Spines were not explicitly modelled but taken into account electrically by modifying the lengths and diameters of the dendrites, using published results, especially in the densely spine-laden middle and distal dendrites, to account for the additional membrane area attributable to the spines (Wolf *et al.* 2005). Being a radially symmetric model, the recordings in this study have been reported from one representative dendrite, responses in the other dendrites being identical.

The model incorporated all the 14 channels known to be present in these neurons. The parameters, except for the time constant of activation of K_{IR} channels, for modelling the different channels were taken directly from Wolf *et al.* (2005). These parameters were obtained from a recent computational study (Steephen and Manchanda 2009), in which the values were derived from rat neurons instead of the non-mammalian *aplysia* neurons as in Wolf *et al.* (2005). Hodgkin–Huxley formulations were used to model the sodium and potassium currents, the level of inactivation in each channel being adjusted using a variable whose value was set to match published data (Wolf *et al.* 2005). The reversal potentials of sodium and potassium channels were taken as +50 mV and −90 mV, respectively. The calcium (Ca^{2+}) currents (N-, Q-, R- and T-types, as well as L-type $Ca_v1.2$ and $Ca_v1.3$) were modelled using the

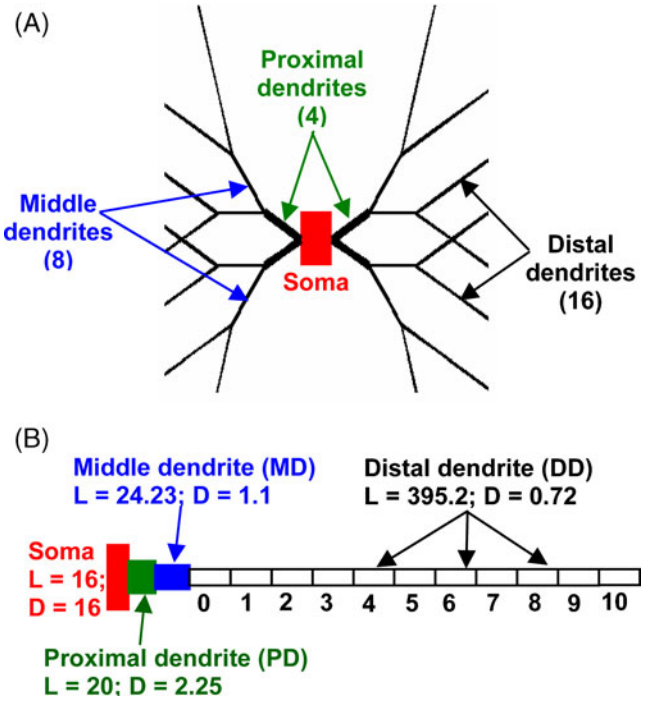

Figure 1. The NAc MS neuron model. (**A**) Detailed view of the radially symmetric model developed in NEURON showing the soma and the different dendrites. (**B**) Compartmentalization of soma and the dendrites in a dendritic branch. Soma and each of the proximal (PD) and middle (MD) dendrites have only one compartment whereas each of the distal dendrites (DD) has 11 compartments (0, 1…10). L and D stand for length and diameter in μm respectively.

Goldman–Hodgkin–Katz (GHK) current equation because of the extremely low intracellular concentration of Ca^{2+}. The intracellular and extracellular concentrations of Ca^{2+} ions were 0.001 mM and 5 mM, respectively. The currents through the Ca^{2+} channels in the model contributed to two different intracellular pools of Ca^{2+}. One pool, to which N-, Q- and R-type Ca^{2+} channels contributed, controlled the Ca^{2+}-dependent K^+ (K_{Ca}) channels, whereas the second pool, to which the other Ca^{2+} channels (T- and L-types) contributed, was only used in the determination of $[Ca^{2+}]_i$ and did not regulate the activity of other membrane channels directly. All the simulations were performed with the cell's operating temperature set to 35ºC. Standard values of membrane capacitance (1 μF/cm^2) and axial resistance (100 Ω-cm) were used. The leak conductance was modelled using the passive channel from NEURON's library with a maximum conductance, $\hat{g}_{pas}=11.5\times10^{-6}$ S/cm^2 and reversal potential, $E_{rev}=-70$ mV.

EPSPs in NAc neurons have been found to be mediated by the activation of both *N*-methyl-D-aspartate (NMDA) and non-NMDA (alpha-amino-3-hydroxy-5-methyl-4-isoxazole

propionic acid; AMPA) receptors (Uchimura *et al.* 1989b; Meredith and Totterdell 1999; Nicola *et al*. 2000; Taverna *et al*. 2004; Carlezon and Thomas 2009). Therefore, the EPSP in our model was generated by a co-localized NMDA-AMPA synapse, modelled using the published data (Wolf *et al.* 2005). The voltage-dependent Mg^{2+} block in NMDA conductance was taken into account while modelling the conductance. 10% of the NMDA and 0.5% of the AMPA currents contributed to Ca^{2+} influx in the pool with which K_{Ca} channels were not associated.

In the studies involving spatiotemporally distributed synaptic inputs, an array of excitatory and inhibitory synapses (a total of 168 synapses) were distributed as per the data obtained from Wolf *et al*. (2005). The excitatory synapses were glutamatergic (NMDA and AMPA) in nature with the reversal potentials set to 0 mV, whereas the inhibitory synapses were gamma amino butyric acid (GABA)-ergic in nature with a reversal potential of −60 mV. The excitatory synapses were placed on the dendrites only, 1 in each of the 4 primary dendrites, 2 in each of the 8 middle dendrites and 4 in each of the 16 distal dendrites. Out of the 84 GABA-ergic synapses, 16 were placed at the soma, 3 in each of the primary and middle dendrites and 2 in each of the distal dendrites. The procedure for applying temporally dispersed, random inputs to the spatially distributed synapses was adopted from literature (Steephen and Manchanda 2009). Each of the excitatory or inhibitory synapses received an independent, probabilistic spike train that was generated with NEURON using the following algorithm. Initially a spike train with a constant interspike interval (ISI) was generated at the required frequency (3 Hz for down-state and 7.5 Hz for up-state). Then, each spike in the train was shifted in time, the amount of shift randomly chosen from a Gaussian distribution with mean=0 and standard deviation 0.25 times the ISI. Finally, the whole of the resulting spike train was once again shifted in time randomly by a value between 0 and the ISI. This entire process was repeated for each of the 168 synapses so as to provide completely random inputs to the different synapses. The NMDA and AMPA conductances at a particular excitatory synapse received identical input trains. As the synaptic drive is modelled as a train of spikes randomized for the arrival time, we performed 30 trials for each study involving synaptic drive to calculate the mean and standard deviation of the data. We performed the Student's *t*-test (paired or independent, as appropriate) in order to statistically compare the relevant sets of data.

The model was validated using data obtained from the literature. For example, the membrane potential responses of the model to somatic current injections (both depolarizing and hyperpolarizing) were nearly identical to those obtained from the published computational model (figure 1D in Wolf *et al.* 2005). Comparison of the temporal characteristics of the EPSPs generated from our model showed similarities with those recorded experimentally (Higashi *et al.* 1989; Pawlak and Kerr 2008). The amplitude of the EPSP in our model was found to be contributed mainly by the AMPARs, as observed experimentally in striatal MS neurons (Pawlak and Kerr 2008). For the synaptic drive case, as the inputs are probabilistic in nature, in order to achieve a robust comparison, we applied the synaptic input train used by Wolf *et al*. (2005) to our model and to the model of Wolf *et al*. (2005) obtained from ModelDB. We found that our model was able to replicate the responses of the Wolf *et al*. model, showing that the model operates identically as in Wolf *et al*. (2005). These similarities of the signals generated in our model with the experimental and computational responses of NAc MS neurons reported in the literature enabled us to place confidence in our model.

The simulations were initiated after a delay of 1000 ms to ensure that the cell had stabilized to a baseline resting potential from which the measurements could be made. In the simulations to study the influence of K_{IR} conductance on subthreshold down-state synaptic inputs (sections 3.2 and 3.3), the depolarization of the resting membrane potential (RMP) of the cell following the modulation of K_{IR} channel conductance was compensated to restore the RMP to its control level (−87.7 mV). This was done by injecting steady hyperpolarizing or depolarizing currents into each compartment of the model cell during the entire duration of the simulation depending on whether the cell was depolarized or hyperpolarized, respectively, following modulation of K_{IR} conductance. The membrane potential compensating currents were obtained from voltage clamp simulations performed to clamp the membrane potential in each compartment to ~ −87.7 mV under resting conditions when the K_{IR} conductance in the model was varied. The parameters of the EPSP compared include its peak amplitude, half width, rise time and decay time. Half width was taken as the time between 50% of the amplitude in the rising and falling phases of the EPSP, rise time as the time taken to rise from 10% to 90% of the EPSP amplitude in the rising phase and decay time as the time taken to fall from 90% to 10% of the EPSP amplitude in the falling phase of the EPSP.

The active conductances were modified in the dendrites only, leaving the somatic conductances unchanged. This was done because the excitatory inputs to the MS neurons terminate at the numerous spines that are positioned on the dendrites of the neuron (Carter *et al.* 2007), while the somata being aspiny (Meredith *et al.* 1992; Meredith and Totterdell 1999) do not receive any significant amount of excitatory input (Meredith *et al.* 2008). Moreover, 94% of the dopaminergic inputs that are capable of modulating the active conductances and excitatory inputs in MS neurons (Nicola *et al.* 2000) contact the dendritic shafts and spines of the neuron (Smith and Bolam 1990; Meredith *et al.* 2008), making the

dendrites the primary target for modulation of ionic conductances in computational studies of this kind.

3. Results

3.1 *Effects of dendritic active conductances on EPSPs*

In order to investigate the effects of active conductances in shaping EPSPs, the EPSP was generated at the middle of the distal dendrite (DD5) and recorded at the soma (henceforth, 'EPSP'). The EPSP in the presence of all dendritic active conductances (henceforth, 'control') was compared with the EPSP in their absence (henceforth, 'passive model'). The results are shown in figure 2A (inset showing the EPSPs overlaid for ease of comparison). Blocking active conductances had two main effects: (i) depolarization of RMP of the cell and (ii) changes in EPSP amplitude and kinetics. The RMP of the cell (−87.7 mV in the control) was depolarized to −76.9 mV in the passive model (figure 2A). As seen in the inset, the absence of dendritic active conductances visibly altered EPSP parameters, its amplitude increasing by 50% and half width by 243%. Overall, thus, it appears that active conductances serve to hyperpolarize the cell membrane and to diminish the amplitude of EPSP while narrowing its time course.

In order to ascertain which set(s) of conductances present in MS neurons were mainly responsible for this modulation, the Na^+, Ca^{2+} and K^+ conductances were blocked serially in the control model (figure 2B). The broad finding was that blocking of Na^+ and Ca^{2+} conductances (labelled '(−Na)' and '(−Ca)' respectively) had no effect on the RMP (figure 2B inset) nor did they produce any appreciable changes in EPSP parameters (figure 2B). In contrast, the absence of dendritic K^+ conductances (labelled '(−K)') depolarized the RMP of the cell to −76.8 mV and affected the EPSP markedly, in the same direction as in the passive model. While the EPSP amplitude was boosted by nearly identical amounts as in the passive model (52%), the half width increased to a somewhat greater extent than in the passive model (266%). These observations indicate that K^+ conductances are the key regulators of the RMP of the cell as well as the efficacy of excitatory synaptic inputs in NAc MS neurons.

By blocking the different dendritic K^+ conductances individually, we next investigated whether some of the dendritic K^+ conductances (K_A, K_{IR} and K_{Ca}) contribute more prominently than the others in determining the EPSP parameters. The results of these maneuvers, displayed in figure 3A–D, showed that the absence of K_{Ca} conductance (labelled '(−KCa)') had no appreciable effect on RMP (figure 3B) and EPSP amplitude and half width (figures 3C and D, respectively), and that the absence of K_A conductance (labelled '(−KA)') affected RMP and EPSP parameters only marginally (0.1 mV depolarization in RMP, 4% increase in EPSP amplitude and 1% increase in EPSP half width). In contrast, blockade of dendritic K_{IR} conductance (labelled '(−KIR)') depolarized the cell markedly (by 7.2 mV) and resulted in large percentage changes in EPSP parameters (amplitude augmented by 34% and half width by 118%). Thus, among the K^+ conductances, K_{IR} appears to exert the dominant influence on RMP and on somatic EPSPs.

Although the K_{IR} conductance emerges as the principal determinant of EPSP indices, the changes induced by block

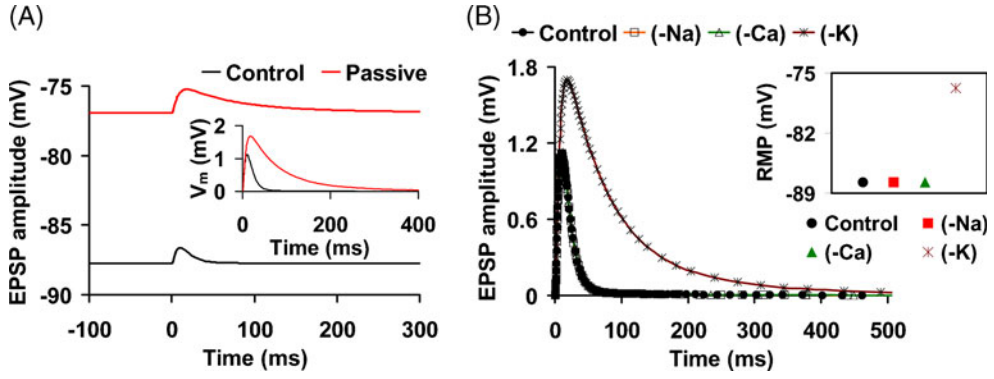

Figure 2. Active conductances, in particular K^+ conductances, modulate RMP of the cell and also the amplitude and kinetics of somatic EPSPs. (**A**) EPSPs from the model with active and passive dendrites showing depolarization of RMP in the passive model (labelled 'Passive') compared to the control (labelled 'Control'). The inset shows the EPSPs overlaid for the ease of comparison of their parameters. EPSP amplitude and half width were augmented upon blocking the active conductances. (**B**) EPSPs on blocking Na^+ [(−Na); unfilled squares] Ca^{2+} [(−Ca); unfilled triangles] and K^+ conductances [(−K); asterisks] compared with the control (filled circles). The inset shows the RMP of the cell corresponding to the EPSPs in (**B**) showing depolarization of RMP upon blocking K^+ conductances. The amplitude and half width of the EPSP were unaffected following the block of Na^+ and Ca^{2+} conductances, but were augmented when K^+ conductances were blocked in the model.

of K_{IR} were markedly lower than those induced by block of all K^+ channels together (compare the bars with forward and backward slanting lines in figures 3C and D), which in turn was similar to those in the passive model. Furthermore, the changes in EPSP parameters following block of all the K^+ conductances together were different from the

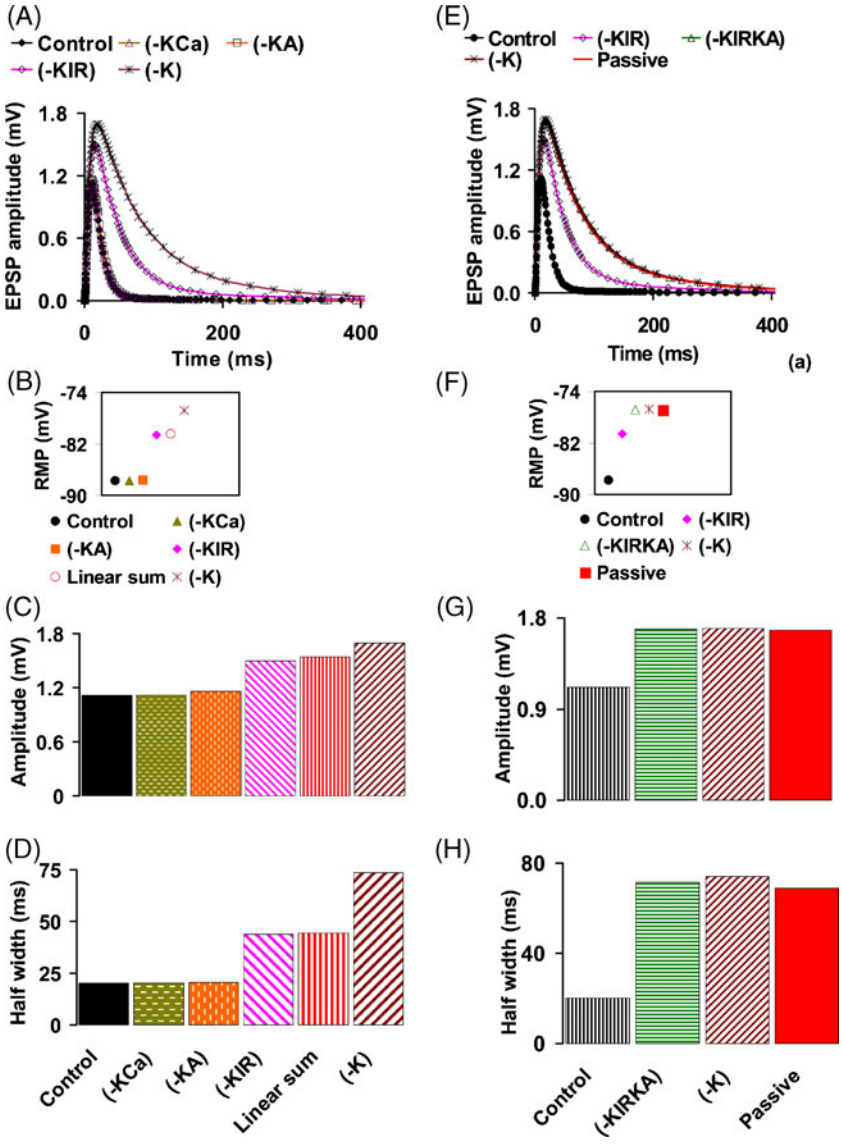

Figure 3. K_{IR} conductance markedly affects the RMP and somatic EPSP parameters in the down-state of NAc MS neurons while K_A conductance contributes only secondarily to these changes when blocked along with K_{IR} conductance. (**A**) EPSPs on blocking individual K^+ conductances. Blocking of the K_{Ca} (unfilled triangles) and K_A (unfilled squares) conductances individually did not produce any notable changes in the EPSP parameters, whereas blockade of K_{IR} conductance alone (unfilled diamonds) changed the RMP and EPSP parameters remarkably. (**B**) RMP of the cell corresponding to EPSPs in (**A**). EPSP amplitude (**C**) and half width (**D**) were enhanced upon blocking K_{IR} (bars with forward slanting lines) and remained more or less unchanged on blocking other K^+ conductances individually (bars with horizontal and vertical dotted lines). Note that the linear sum of the changes in EPSP parameters due to block of K^+ conductances individually (bars with vertical lines) was not equal to the changes observed when all the potassium conductances were blocked together (bars with backward slanting lines). (**E**) EPSPs when K_A and K_{IR} conductances are blocked simultaneously (unfilled triangles), upon blocking all K^+ conductances (asterisks) and in passive model (plain line) compared with the control (filled circles) as well as K_{IR} blocked (unfilled diamonds) conditions. (**F**) RMP of the cell corresponding to EPSPs in (**C**). Upon simultaneous blocking of K_A and K_{IR} conductances (bars with horizontal lines) the EPSP amplitude (**G**) and half width (**H**) rose from the control (bars with vertical lines) and these changes were approximately equal to those when all K^+ conductances were blocked simultaneously (bars with backward slanting lines) and also in passive model (filled bars).

linear sum of changes (labelled 'Linear sum') due to block of K^+ conductances individually (compare the bars with backward slanting lines and vertical lines in figures 3C and D). It was, therefore, speculated that along with K_{IR} conductance, some other active conductance(s) might secondarily be playing a role in altering the EPSPs, ensuing from the primary changes induced by K_{IR}.

In order to investigate this idea, each of the different active conductances was blocked in the model in combination with K_{IR} conductance. In this case too, none of the Na^+ and Ca^{2+} conductances nor the K_{Ca} conductance had any discernable influence on RMP and EPSP parameters (data not shown). However, as shown in figure 3E–H, when K_A and K_{IR} conductances were blocked simultaneously (labelled '(−KAKIR)'), the changes in the RMP (figure 3F) and EPSP parameters (figures 3G and H) were roughly equal to the changes resulting from simultaneous block of all the K^+ conductances. This implies that even though the individual contribution of K_A channels to RMP and to EPSP indices is negligible, K_A conductance also influences these parameters in combination with K_{IR}. We analysed this situation and found that due to the depolarization in the RMP brought about primarily by the block of K_{IR} conductance, the cell is driven into the voltage range of activation of K_A channels, evoking an outward current that diminishes the amplitude and temporal characteristics of the EPSP. Blocking K_A channels along with K_{IR} raises the amplitude and time course of the EPSP and causes the depolarization of the RMP as well.

As observed above, depolarization induced by blocking of K_{IR} can entrain other active conductances (principally the K_A) which secondarily affect the EPSPs. Because of the non-linear interactions between the several active channels present in the model, there could conceivably be secondary effects on the EPSPs such as those mediated by K_A channels, as indicated by figure 3E–H. Therefore, in order to isolate the effects of K_{IR} and minimize as far as possible the effects of other conductances, we restored the membrane potential to the resting level (−87.7 mV) by injecting suitable hyperpolarizing or depolarizing currents into the model. Such protocols have previously been adopted in studies aimed at isolating the effects of a single conductance out of the many present in a neuron (e.g. Magee (1998) for the case of the I_h conductance known to regulate the resting potential and influence EPSP parameters in hippocampal pyramidal neurons). The EPSPs in three conditions – (i) control, (ii) RMP unrestored and (iii) RMP restored conditions – were recorded and are shown in figure 4A. We found that the direction of changes in EPSP parameters (amplitude, half width, rise time and decay time) was similar in both RMP unrestored and restored conditions, but the extent of changes was enhanced when RMP was restored (figure 4B–E). We found that this is due to the reduction in the activation of outward K_A currents when the membrane potential was restored. The percentage increases in the different EPSP parameters from the control under RMP unrestored and restored conditions are provided in figure 4B–E. The figures also show that the enhancement in the half width of the EPSP from the control upon blocking of K_{IR} is mainly due to the enhancement in decay time (292% under RMP restored conditions), the increase in rise time being comparatively minor (40% under RMP restored conditions).

Earlier studies (Wilson 1992, 1993) suggest that while the K_{IR} conductance is a major determinant of the membrane potential and EPSP parameters in the down-state, in the up-state of the neuron, the K_A conductance, in particular K_{As}, might play a bigger part in shaping EPSPs (Nisenbaum *et al.* 1994, Mahon *et al.* 2000a, b). Therefore, we investigated the role played by the K_{As} conductance by measuring its effects on EPSPs generated at depolarized potentials akin to physiological up-state potentials (~ –65 mV, obtained by injecting depolarizing currents). Table 1 shows the percentage increase in the EPSP amplitude and half width when K_{IR} and K_{As} conductances were blocked individually in the resting (–87.7 mV) and at depolarized membrane potential (–65 mV). As is evident from table 1, in the down-state, the EPSP amplitude and half width increased by 64% and 160%, respectively, when K_{IR} was blocked, whereas the blocking of K_{As} had no effect on EPSP amplitude and produced only a 5% rise in the EPSP half width. However, when the membrane potential was depolarized to –65 mV, the contribution from K_{As} conductance was markedly boosted, EPSP amplitude increasing by 24% and half width by 191% when K_{As} conductance was blocked. In contrast, the blocking of K_{IR} increased the amplitude only by 7% and decreased half width by 26%. Thus, we find that while the K_{IR} conductance is the major determinant of membrane potential and EPSP parameters in the down-state, in the up-state, the K_{As} conductance plays a more prominent role in shaping the EPSPs.

The salient observations arising from a consideration of the above data are (i) that K_{IR} conductance in NAc MS neurons primarily, and significantly, influences the shaping of somatic EPSPs in the down-state and (ii) that progressive depolarization of the membrane potential could result in increasing influence of K_A conductance in shaping the somatic EPSPs. In the following section, we investigate the modulation of subthreshold synaptic inputs by the K_{IR} conductance in detail.

3.2 *Effects of modulation of K_{IR} conductance on EPSP properties*

Physiologically, the conductance of K_{IR} channels is likely to be modulated by external factors such as dopamine, a major neurotransmitter carrying information about reward

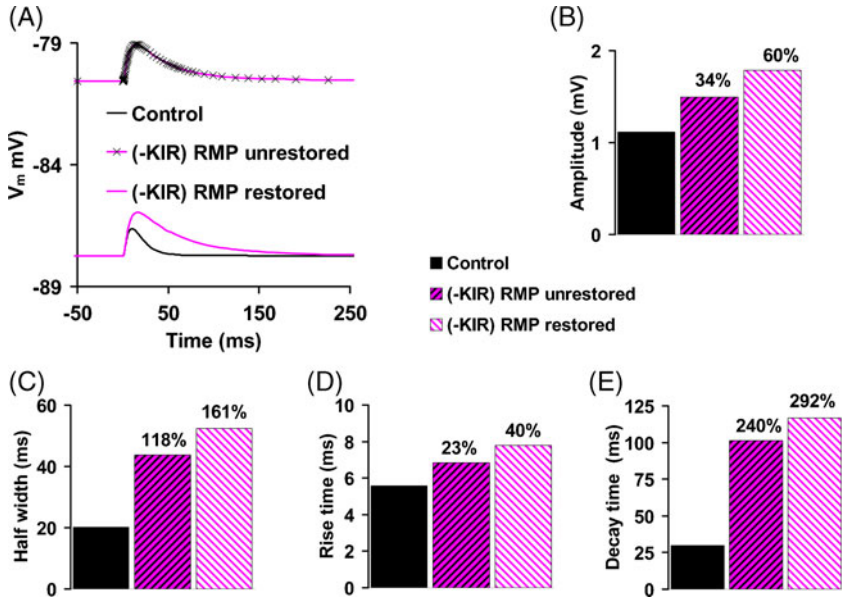

Figure 4. Restoration of RMP during blocking of K_{IR} conductance further enhanced the EPSP parameters. (**A**) EPSPs in the control, RMP unrestored and RMP restored conditions. Blocking of K_{IR} conductance depolarized the membrane potential by 7.2 mV (light line with crosses) compared to the control (dark line). The direction of changes in EPSP parameters were preserved upon restoration of RMP. The changes in EPSP amplitude (**B**), half width (**C**), rise time (**D**) and decay time (**E**) upon blocking K_{IR} conductance under RMP unrestored conditions (bars with backward slanting lines) in the model compared to the control (filled bars) was enhanced further upon restoration of the RMP (bars with forward slanting lines).

conditions to the NAc (Uchimura *et al*. 1989a; Moyer *et al*. 2007). Therefore, we investigated the effects of varying the maximum conductance of K_{IR} channels ($g_{max}(K_{IR})$) on somatic EPSP parameters as well as the probable mechanisms underlying these effects. Figure 5A shows the EPSPs generated from our model for different levels of $g_{max}(K_{IR})$ under RMP unrestored conditions, while the inset shows the amplitude of the EPSPs after restoration of RMP. Figure 5A, as expected, shows that reduction in $g_{max}(K_{IR})$ resulted in progressive depolarization of the RMP. As shown in the inset, reduction in $g_{max}(K_{IR})$ enhanced the amplitude and temporal characteristics of the EPSP (also see Table 2). The simulations reported in the next three sections (3.3 to 3.5) were again done after restoring the RMP to isolate the effects due to K_{IR} conductance (see the section on methods).

Table 1. Percentage increases in EPSP amplitude and half width at down-state (−87.7 mV) and up-state (−65 mV) membrane potentials when K_{IR} and K_{As} are blocked individually

	EPSP amplitude (mV)		EPSP half width (ms)	
V_m (mV)	($-K_{IR}$)	($-K_{As}$)	($-K_{IR}$)	($-K_{As}$)
−87.7	64	0	160	5
−65	7	24	−26	191

3.3 *Effects of modulation of K_{IR} conductance on electrical properties of the cell membrane*

The changes in EPSP parameters observed here could be attributed to the changes in the electrical properties of the cell membrane following the modulation of K_{IR} conductance. For instance, suppression of K_{IR} conductance is expected to lead to a rise in both the input resistance (R_{in}) of the cell and its effective membrane time constant [τ_m; we have used the descriptor 'effective' here because of the presence of voltage gated channels in the dendrites (Koch *et al.* 1996), which endow an active component to electrical responses of the membrane even in the subthreshold region]. In order to analyse the mechanisms underlying the changes in EPSP parameters, we measured R_{in} and τ_m. R_{in} was obtained from the slope of the I-V curve of the cell at different levels of $g_{max}(K_{IR})$. In order to plot the I-V curves, step currents were injected into the cell at the distal dendritic location (DD5). The currents injected ranged from −0.064 to +0.064 nA in 17 equal steps for a duration of 1500 ms (inset of figure 5B shows the response of the model to step current injection of −0.04 nA under different $g_{max}(K_{IR})$ conditions). The low amplitudes of

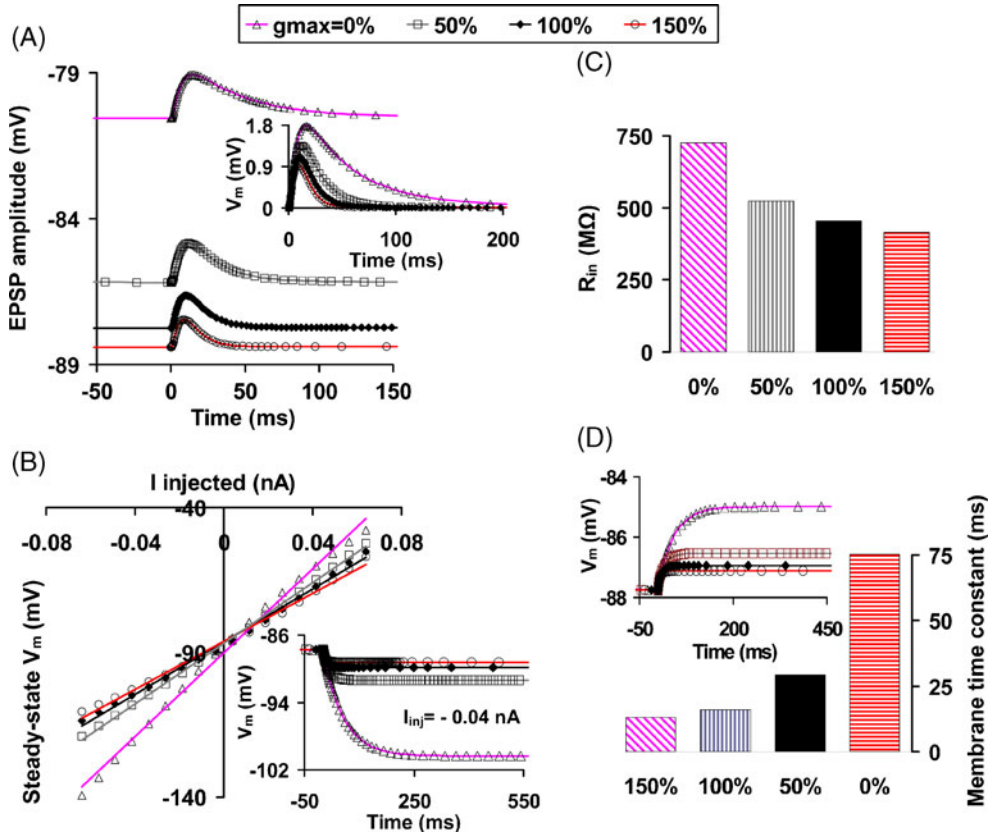

Figure 5. Changes in K_{IR} conductance modulate somatic EPSPs and electrical properties of the cell membrane. (**A**) EPSPs from our model under different levels of $g_{max}(K_{IR})$ showing depolarization of RMP under reduced $g_{max}(K_{IR})$ conditions. Inset shows the EPSPs under RMP restored conditions illustrating that their amplitude and time course enhanced with reduction in $g_{max}(K_{IR})$. (**B**) Plots of I-V curves from the model under different levels of $g_{max}(K_{IR})$ fitted with best-fit straight lines to measure R_{in}, the slope of the I-V curves. The inset shows the response of the model to a hyperpolarizing current injection (−0.04 nA for 1500 ms), both current injection and recording at DD5. (**C**) Reduction in $g_{max}(K_{IR})$ raised the input resistance of the cell. (**D**) Effective τ_m rose with reduction in K_{IR} conductance. The inset shows the somatic response of the model to a depolarizing somatic current injection (0.01 nA for 1500 ms) under different levels of $g_{max}(K_{IR})$.

Table 2. Summary of the values of RMP, parameters of the somatic EPSP and membrane properties for different levels of $g_{max}(K_{IR})$

Parameters		$g_{max}(K_{IR})$=0%	$g_{max}(K_{IR})$=50%	$g_{max}(K_{IR})$=100%	$g_{max}(K_{IR})$=150%
RMP (mV)		−80.56	−86.19	−87.74	−88.4
Amplitude (mV)		1.79	1.36	1.12	0.95
Half width (ms)		52.4	28.4	20.1	18.3
Rise time (ms)		7.8	6.1	5.6	4.9
Decay time (ms)		116.8	45.2	29.8	23.7
R_{in} (MΩ)		725	523	455	414
τ_m (ms)		75.2	29.3	16.1	13.1
Half attenuation distance (μm)	DD10	245	205	190	178
	DD5	160	127	118	111

the currents ensured that the changes in membrane potential were confined to ranges of linear behaviour. For each value of the current injected, the steady-state membrane potentials were recorded at the site of current injection and the data thus obtained were plotted and fitted with best-fit straight lines (figure 5B).

As shown in figure 5C, R_{in} varied inversely with $g_{max}(K_{IR})$. Under control conditions R_{in} was 455 MΩ (R^2=0.99, the high value of R^2 indicating that the cell membrane was passive and operating in the linear range) and rose to 725 MΩ (R^2=0.99) in the absence of K_{IR} currents (also *see* table 2). This elevated R_{in} may underlie the enhancement of EPSP amplitude following the reduction in K_{IR} conductance. τ_m was evaluated as the time taken to reach 84% of the steady-state somatic response of the model (inset of figure 5D) to a sufficiently long-duration step current injection at the soma (0.01 nA for 1500 ms). The index 84% was taken from the standard definition of membrane time constant at the point of current injection (in an infinite cable) as predicted by the solution of the cable equation (Johnston and Wu 1995). τ_m also showed inverse relation with $g_{max}(K_{IR})$, absence of K_{IR} current resulting in τ_m nearly 4.7-fold higher than the control (figure 5D; also *see* table 2). The augmentation of τ_m appears to cause the slow rise and fall of the EPSP under reduced $g_{max}(K_{IR})$ conditions.

3.4 *Effects of modulation of K_{IR} conductance on EPSP propagation and spatial electrical properties of the cell membrane*

Figures 6A–D show the EPSPs generated at the distal end of the distal dendrite (DD10) and recorded at different locations along the length of the dendrite. We found that the amplitude of the local EPSP increases with reduction in $g_{max}(K_{IR})$. Additionally, for all levels of $g_{max}(K_{IR})$, the majority of the reduction in amplitude of the EPSP occurs in the distal dendrite (~ 90% at DD0) and only about 5–6% of the reduction occurs in its further propagation towards the soma. The enhancement in membrane resistance upon reduction of K_{IR} conductance might result in differences in the spatial electrical properties of the membrane. One such possibility is a change in the rate of voltage attenuation along the length of dendrite. This possibility was tested by injecting a sufficiently long-duration step current (0.01 nA for 1500 ms) at the tip of the distal dendrite (DD10). As a measure of spatial spread, we used the index of steady-state voltage attenuation, obtained by plotting the steady-state voltage reached in each dendritic location as a function of distance from the soma. In figure 6E, the steady-state voltage at each location is shown normalized with respect to that at the current injection site for different levels of $g_{max}(K_{IR})$. The half-attenuation distance, which is the distance at which the voltage attenuation is 50%, varied inversely with $g_{max}(K_{IR})$, being 190 μm under control conditions and rising to 245 μm in the absence of K_{IR} conductance (indicated by lines in figure 6E and also table 2). Changing the site of current injection from DD10 to DD5 in order to reduce end effects (e.g. current reflection from the electrically sealed tip of the dendrite) also showed similar results (half-attenuation distance rising from 118 μm in the control to 160 μm under K_{IR} blocked conditions; figure 6F; also table 2).

Thus, we found that modulation of the amplitude and kinetics of subthreshold somatic EPSPs by the K_{IR} conductance were accompanied by the modulation of electrical properties of the cell membrane such as R_{in} and τ_m and also the changes in the spatial electrical properties of the neuronal membrane, effects that are consistent with the electrotonic expansion of the dendrite earlier investigated (Wilson 1995).

3.5 *Effect of K_{IR} conductance on normalization of synaptic inputs at the soma*

It has been found that in central neurons dendritic voltage-gated ion channels serve to counter the passive filtering of EPSPs as they propagate towards the soma, thereby assisting in the normalization of these inputs at the soma irrespective of the site of their generation (Magee and Cook 2000; Williams and Stuart 2003). We explored if EPSPs under control conditions undergo normalization in MS neurons. As K_{IR} is a major conductance affecting the EPSPs in the down-state of the neuron, we also investigated whether K_{IR} contributes to this normalization. Figures 7A and B show the local dendritic EPSPs and propagated somatic EPSPs, respectively, generated at distal (DD5; light trace with unfilled circles) and proximal (PD; dark trace with asterisks) dendritic locations. The local dendritic EPSP at the distal location was found to be 7.4 times larger than that at the proximal location, whereas somatic EPSPs propagated from distal and proximal locations were relatively similar in amplitude (with EPSP from proximal location being only 0.7 times larger that from the distal location). The amplitude of the local dendritic EPSPs for different values of $g_{max}(K_{IR})$ was plotted along the length of the dendrite (figure 7C). We find that, in the control conditions (filled diamonds), the amplitude of the local dendritic EPSP from distal location (DD10) increases more than 11-fold compared to that from the proximal location (PD). However, when these EPSPs are recorded at the soma (figure 7D), they show relatively similar amplitudes, only a 52% reduction in amplitude when the location of EPSP generation is moved from the proximal to the distal location. Furthermore, figure 7D shows that the extent of normalization was dependent on K_{IR} density, progressive reduction in $g_{max}(K_{IR})$ leading to a progressive enhancement of amplitude

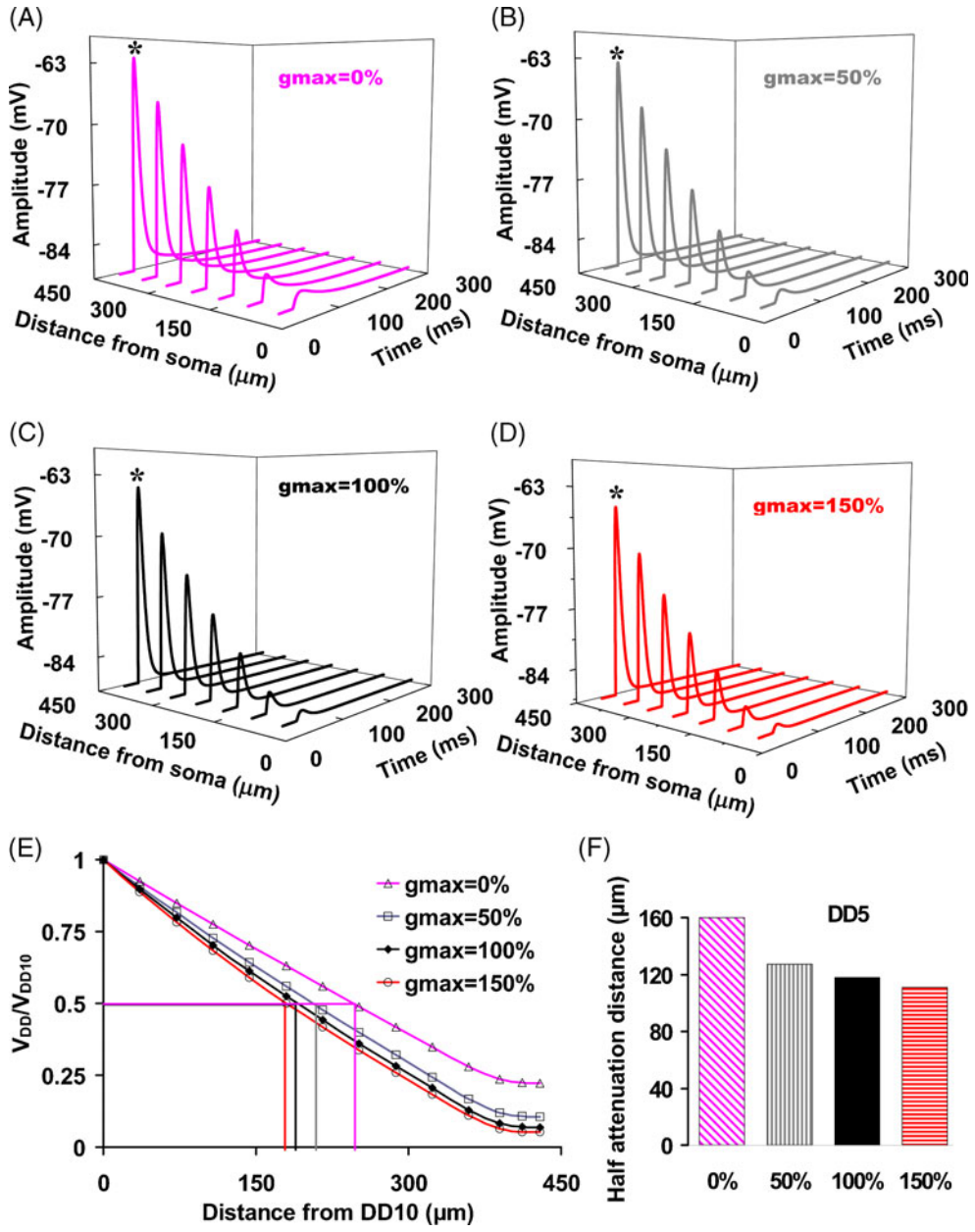

Figure 6. K_{IR} conductance modulates local EPSPs and the spatial electrical properties of the cell membrane. (**A**–**D**) EPSPs generated at DD10 (indicated by asterisks) and recorded at different distances (DD10, DD8, DD6, DD4, DD2, DD0 and soma). See text for details. (**E**) The steady-state voltage at each location along the dendrite normalized to that at the site of current injection (DD10) plotted as a function of distance from the soma under different levels of $g_{max}(K_{IR})$. (**F**) Half-attenuation distance varied inversely with K_{IR} conductance when the site of current injection was at DD10 (marked using lines in (**E**)) and at DD5 (**F**) as well.

normalization at the soma. The percentage decrease in amplitude of propagated somatic EPSP from the distal location (DD10) compared with that from the proximal location (PD) was 31% with K_{IR} conductance blocked and it rose to 58% for $g_{max}(K_{IR})$ set to 150%. This enhancement in the extent of amplitude normalization with reduction in $g_{max}(K_{IR})$ could be attributed to the increase in the amplitude of the local dendritic EPSPs at the distal locations when $g_{max}(K_{IR})$ is reduced. These simulations show that normalization of EPSP amplitude at the soma does take place to a significant degree in our NAc MS neuron model, the extent of normalization being dependent on the level of K_{IR} conductance.

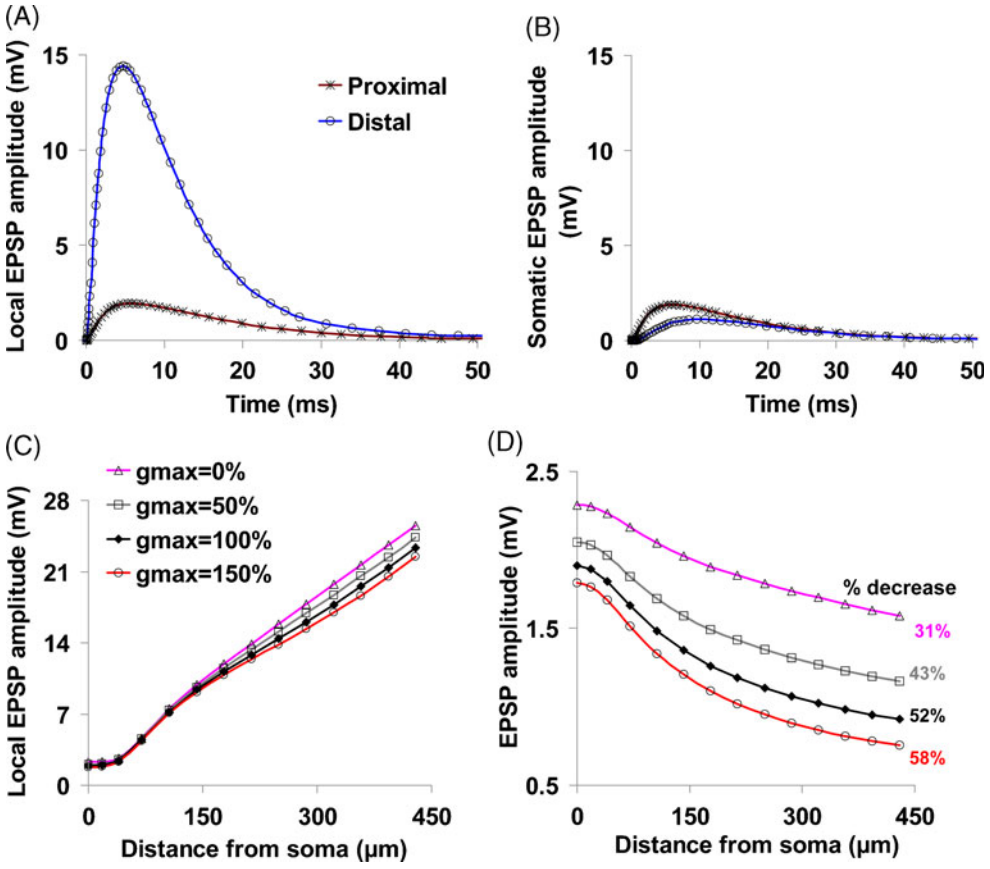

Figure 7. K_{IR} conductance contributes to normalization of amplitude of synaptic inputs at the soma. Local dendritic EPSPs (**A**) and propagated somatic EPSPs (**B**) generated at a proximal (PD; asterisks) and distal (DD5; unfilled circles) dendritic locations. Note the large amplitude changes in the local dendritic EPSPs from the two locations at different distances from the soma and similar amplitude of the propagated EPSPs at the soma. Peak amplitude of the local dendritic (**C**) and propagated somatic (**D**) EPSPs plotted against the distance from the soma for different levels of $g_{max}(K_{IR})$. Reduction in $g_{max}(K_{IR})$ enhanced the amplitude of the local EPSPs at the distal dendritic locations while it also enhanced the extent of normalization of amplitude of synaptic inputs at the soma.

3.6 *Effects of modulation of K_{IR} conductance on cell excitability*

The studies presented so far suggest that K_{IR} conductance affects the amplitude and time course of EPSPs in such a way that more effective summation should occur when $g_{max}(K_{IR})$ is reduced. This, in turn, should lead to an increase in the excitability of the cell. To test this prediction, we need to allow the membrane potential to change beyond the limited window of V_m close to the hyperpolarized down-state potential explored above. Therefore, we next carried out studies in the absence of compensating current injection, allowing membrane potential to depolarize following the block of K_{IR}. We investigated, for different values of $g_{max}(K_{IR})$, the spiking behaviour of the cell following two kinds of stimulation: (i) injection of rectangular pulses of current at the soma and (ii) spatiotemporally distributed synaptic drive mimicking the physiological inputs.

In current injection studies a rectangular current pulse of amplitude 0.25 nA for 500 ms, which elicits two spikes in control conditions was injected into the soma of the model cell. As shown in figure 8A, when the conductance of the K_{IR} channel was elevated ($g_{max}(K_{IR})$=150%), the cell produced no spike, whereas the same current produced progressively increasing number of spikes when $g_{max}(K_{IR})$ was reduced. Figure 8B summarizes this data showing that number of spikes increased with reduction in $g_{max}(K_{IR})$. Table 3 shows that the latency to the first spike increased with $g_{max}(K_{IR})$, thus indicating that K_{IR} conductance acts to increase the duration of the depolarizing ramp before firing the action potential, as also suggested by previous computational studies (Moyer *et al*. 2007; Steephen and Manchanda 2009).

Spatiotemporally distributed synaptic inputs at a mean frequency of 3 Hz per synapse for the down-state and 7.5 Hz per synapse for driving the cell to up-state as

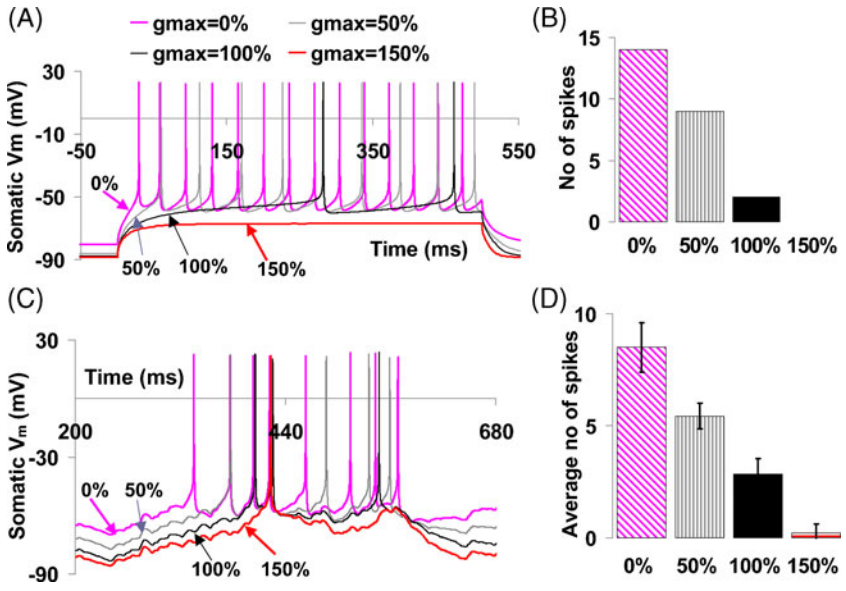

Figure 8. Cell spiking enhances with reduction in K_{IR} conductance. (**A**) Response of the model to step current injections of 0.25 nA for 500 ms at the soma for different levels of $g_{max}(K_{IR})$. (**B**) Bar graph showing reduction in the number of spikes when $g_{max}(K_{IR})$ is raised. (**C**) Response of the model to spatiotemporally distributed synaptic inputs of frequency 3 Hz in the down-state and 7.5 Hz to drive the cell to up-state for different values of $g_{max}(K_{IR})$. Note the depolarization in the down-state potential of the cell with decrease in $g_{max}(K_{IR})$. (**D**) The average number of spikes varies inversely with $g_{max}(K_{IR})$. Mean number of spikes for each $g_{max}(K_{IR})$ value shown (0%, 50%, 100% and 150%) was significantly higher ($P<0.001$) than the next.

described in Steephen and Manchanda (2009) were applied to the model for different values of $g_{max}(K_{IR})$. The responses are shown in figure 8C. Note that the mean down-state potential in control conditions (−80 mV) is ~7 mV depolarized compared with the RMP without synaptic input (−87.7 mV), essentially because of the net excitatory drive. As K_{IR} conductance was reduced, the down-state potential was further depolarized, whereas enhancement of K_{IR} conductance (to 150% of control) hyperpolarized the membrane potential by 3 mV. Moreover, cell excitability was enhanced with progressively greater number of spikes being generated as $g_{max}(K_{IR})$ was progressively reduced. Figure 8D shows the average number of spikes (30 trials) for different levels of $g_{max}(K_{IR})$. We found that the average number of spikes increased with reduction in $g_{max}(K_{IR})$ and the difference in means were statistically significant (paired *t* test; $P<0.001$). Table 3 shows that, as in the case of current injection study, the onset time for the first spike increased with $g_{max}(K_{IR})$. For the reduced $g_{max}(K_{IR})$ and control conditions, the model generated spikes and the differences in means of the onset time of the first spike were found to be statistically significant using the paired *t*-test ($P<0.001$). However, in the case of enhanced $g_{max}(K_{IR})$, where the cell generated spikes very rarely, we performed independent *t*-tests to compare the differences in means and these were again found to be significantly different ($P<0.001$).

3.7 *Effects of modulation of K_{As} conductance in relation to K_{IR} on cell excitability*

In order to study the role of K_{As} in relation to K_{IR} in determining the spiking behaviour of the neuron in the up-state, we performed both current injection as well as synaptic input simulations after allowing the membrane to depolarize in response to a reduction in K_{IR} conductance. We chose a level of $g_{max}(K_{IR})$ (50% of control) that depolarized the membrane by a moderate amount and evoked a significant level of spiking in response to either current injection (9 spikes for a somatic current injection of 0.25 nA for 500 ms) or increase in synaptic drive (6 spikes). In the current injection study, reduction of $g_{max}(K_{IR})$ to 50% of its control level depolarized the resting membrane from −87.7 mV to ~ −86 mV. The

Table 3. Changes in onset time of the first spike with $g_{max}(K_{IR})$

	Onset time of first spike (ms)	
$g_{max}(K_{IR})$	Current injection	Synaptic input (30 trials)
0%	29	33±13
50%	60	70±27
100%	282	128±47
150%	–	237±50

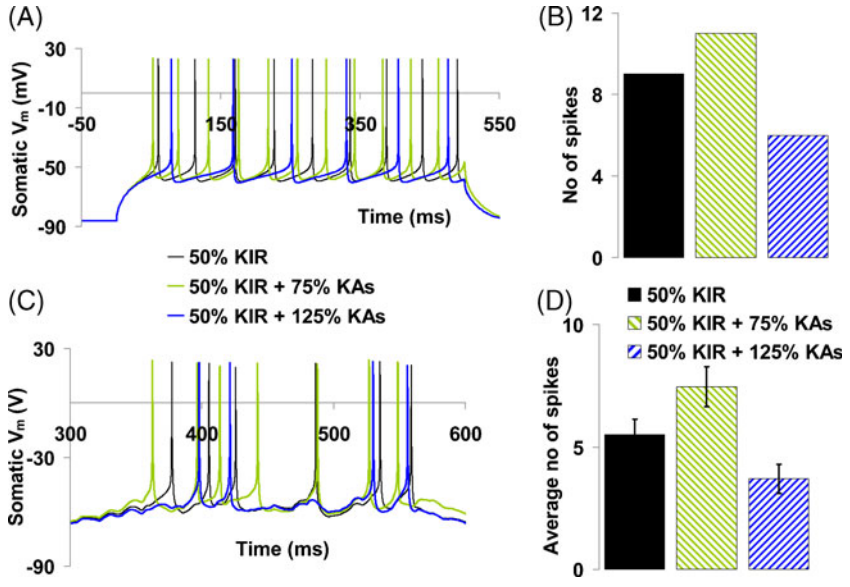

Figure 9. K_{As} conductance also contributes to the increase in spiking behaviour of MS neurons. (**A**) Response of the model to current injection of 0.25 nA for 500 ms at the soma under conditions of concomitant changes in K_{IR} and K_{As} conductances, when the K_{IR} conductance is reduced to 50% (thin black trace), when the K_{As} conductance is additionally reduced to 75% (thick green trace) and to 125% (thick blue trace). (**B**) Bar graph showing the number of spikes generated when the K_{IR} conductance is reduced to 50% (filled bars) when the K_{As} conductance is additionally reduced to 75% (forward slanting lines) and increased to 125% (backward slanting lines). (**C**) Response of the model to spatiotemporally distributed synaptic inputs under conditions described in (**A**). (**D**) Bar graph showing the number of spikes generated under the same conditions as in (**B**).

response for this level of $g_{max}(K_{IR})$ is shown in figure 9A (thin black trace). Keeping $g_{max}(K_{IR})$ at 50% we either increased or decreased the K_{As} conductance to 75% and 125% of its control value and measured the corresponding responses. These are indicated respectively by the thick green and blue traces in figure 9A. Figure 9B shows the bar graph for the number of spikes when the K_{IR} conductance was reduced to 50% (filled bars) when the conductance of K_{As} was additionally reduced to 75% (forward slanting lines) and when K_{As} conductance is additionally increased to 125% (backward slanting lines). As is evident from figures 9A and B, suppression of the K_{As} conductance resulted in a marked increase in the spiking frequency while elevation of K_{As} had the opposite effect. A drop in K_{As} conductance also elicited a reduction in the latency to the first spike, as demonstrated by the data in table 4.

In the case of synaptic drive, reducing $g_{max}(K_{IR})$ to 50% depolarized membrane to −74 mV at the basal level of spatiotemporally distributed synaptic activation (3 Hz, giving rise to the noisy down-state under synaptic drive visible in figure 9C). Figure 9C shows the spiking behaviour of the neuron for the following conditions: $g_{max}(K_{IR})$=50% (thin black trace), K_{As} conductance additionally reduced to 75% (thick green trace) and K_{As} conductance additionally increased to 125% (thick blue trace). Figure 9D shows the bar graph for the number of spikes in each of these cases. These figures indicate that, as in current injection study, reduction of K_{As} conductance markedly increased the spiking frequency and reduced the latency to the first spike (table 4), while elevation of K_{As} had the opposite effects. Each of these effects was statistically significant (paired *t*-test; $P<0.001$). Reduction or enhancement of K_{As} conductance to different degrees resulted in effects in the expected direction and proportional to the extent of block or enhancement of the conductance. Taken together, these findings indicate that, unlike in the down-state, where K_{IR} is the primary controller of electrical behaviour of the neuron, at depolarized levels of membrane potential both K_{IR} and K_{As} conductances affect the neuronal excitability to substantial degrees.

Table 4. Influence of varying K_{As} conductance along with 50% $g_{max}(K_{IR})$ on onset time of the first spike

	Onset time of first spike (ms)	
$g_{max}(K_{As})$	Current injection	Synaptic input (30 trials)
100%	60	72±27
75%	52	53±16
125%	79	91±38

4. Discussion

In this study we have shown that, first, dendritic active conductances are strong modulators of subthreshold excitatory synaptic inputs in NAc MS neurons and, second, among the conductances present in the neuron, K_{IR} conductance is the primary determinant of the RMP and somatic EPSPs in the down-state. The excitatory effects evoked in the cell following the reduction in K_{IR} conductance were accompanied by an increase in R_{in} and τ_m as well as spatial electrical properties such as the half attenuation distance. Owing to the depolarization of the RMP evoked by the blockade of K_{IR}, the K_A conductance also affected the EPSPs secondarily. Our results suggest that K_{IR} and K_{As} channels in NAc MS neurons influence the modulation of temporal integration as well as the firing properties of the neuron, the membrane potential of their operation being different.

It may be noted that although the effects of K_{IR} and K_{As} in determining the membrane electrical properties in MS neurons have been investigated earlier, our findings extend previous studies in the field in several ways: (i) Computational studies done previously in striatal MS neuron investigating the role of K_{IR} channels in the modulation of membrane electrical properties (Wilson 1992,1993) used a reduced biophysical model of the neuron in which the only conductances present were the K_{IR} and leak conductances. While these studies demonstrated a marked effect of the K_{IR} conductance on generation and propagation of synaptic potentials, the question remained as to whether these effects would also occur in a physiologically more realistic model of an MS neuron equipped with its wide array of voltage-dependent active channels. The presence of a large number of nonlinear conductances makes it difficult to predict such effects analytically, and complex interactions between these mechanisms can sometimes lead to counter-intuitive outcomes (Williams and Stuart 2003; Samuelsson and Kotaleski 2007; Steephen and Manchanda 2009). We, therefore, used a biophysically detailed model of the NAc MS neuron, which has recently become available (Wolf *et al*. 2005), incorporating all the 14 active conductances known to be present in these neurons, to investigate the effects of these active conductances in modulating the subthreshold down-state synaptic inputs as well as excitability in the up-state. In a related context, the outcomes of our study are closer to the physiological situation also because we have used more realistic models of NMDA-AMPA synapses for the generation of EPSP rather than the generalized alpha synapse. (ii) Previous computational studies on the subject (Wilson 1992, 1993) excluded other active conductances from the model in order to isolate the effects due to K_{IR}. However, in our model we have taken a different approach, i.e. while we included all the known active conductances, we isolated the effects due to K_{IR} by restoring the RMP electrically to its resting value (~ −87.7 mV), a maneuver that would ensure primarily the activation of K_{IR} conductance. Restoration of RMP in order to selectively study the effects of a single conductance, e.g. due to I_h currents in hippocampal pyramidal neurons, has been employed in previous studies also (Magee 1998). (iii) We have investigated the effects of the K_{IR} conductance on normalization of synaptic potentials as well as on the spiking behaviour of the neuron through current injection and synaptic input studies, effects that have not previously been explored. (iv) Finally, as the K_{As} conductance is suspected to play a major role in the up-state of the neuron, we investigated the role of K_{As} in relation to K_{IR} in modulating up-state EPSPs as well as spiking behaviour of the cell. We discuss below (i) the influence of K_{IR} and K_{As} channels on MS neuron membrane biophysics and (ii) the implications for MS neuron functioning in the context of synaptic input processing.

4.1 *Influence of K_{IR} and K_{As} on MS neuron membrane biophysics*

K_{IR} channels present in NAc MS neurons have been suggested to be crucial determinants of resting potential of the cell (Uchimura *et al.* 1989a; Uchimura and North 1990; Mermelstein *et al.* 1998). In other cell types such as cardiac cells and skeletal muscle cells, these channels provide large inward currents at membrane potentials more negative than the reversal potential of K^+ (E_K=−90 mV), thus preventing excessive hyperpolarization of the resting potential caused by the electrogenic Na^+ pump. Additionally, in the event of small depolarizations they provide small outward currents, thus stabilizing the resting potential of the neuron at a hyperpolarized potential near to E_K (Kubo *et al.* 1993; Hille 2001). Depolarization of RMP following the reduction of K_{IR} conductance has been suggested to occur in NAc MS neurons (Uchimura *et al.* 1989a; Perez *et al.* 2006). Supporting this idea, our simulations show that K_{IR} currents act to maintain the RMP (~ −88 mV) in NAc MS neurons, their absence depolarizing the cell by about 7 mV. Dopamine-induced membrane potential changes (~ 6 mV) have been reported in literature apparently mediated by unidentified K^+ channels active in the resting conditions of NAc MS neurons (Uchimura *et al*. 1986; Higashi *et al*. 1989; Uchimura and North 1990; Nicola *et al*. 2000).

Alterations in the magnitude of K_{IR} conductance are believed to have major impact on the response of MS neurons to excitatory inputs (Wilson and Kawaguchi 1996; Mermelstein *et al.* 1998). K_{IR} currents, comprising the major portion of the currents active in the down-state of the neuron (Nisenbaum and Wilson 1995), are found to be

critical in determining its input resistance in the quiescent state (Wilson and Kawaguchi 1996). The presence of these currents reduces the membrane resistance in MS neurons (North and Uchimura 1989), thus resisting attempts by excitatory synaptic inputs to depolarize the membrane potential (Wilson and Kawaguchi 1996) and resulting in low-amplitude EPSPs. In agreement with these predictions, our results showed that the suppression of K_{IR} conductance increased the amplitude of EPSPs that was accompanied by a rise in R_{in}. The depolarization of the RMP and enhancement of R_{in} would together facilitate the transition of the neuron from the down-state to the up-state. Additionally, a reduced K_{IR} conductance enhanced the membrane time constant ($\tau_m = R_m C_m$) that might be due to the increase in membrane resistance. This in turn would result in a slower decay of the injected current, prolonging the time course of the EPSP that was manifested in our simulations. This augmentation of the amplitude as well as the time course of the EPSPs reaching the soma would facilitate enhanced temporal summation of these inputs at the soma, thus increasing the effectiveness of these inputs during synaptic integration and consequently, of the likelihood of cell firing.

K_{IR} channels in MS neurons share certain important electrical characteristics with I_h channels present in the dendrites of hippocampal and neocortical pyramidal neurons. The currents through both the channels are activated by hyperpolarization, with hyperpolarization increasing the inward currents through them. Both currents are non-inactivating as well. Larger depolarization deactivates these currents, thus blocking them near the firing threshold (Mermelstein *et al.* 1998; Magee 1998). The presence of I_h channels modulates the resting potential, hyperpolarizing the RMP, and decreases the amplitude and duration of the EPSP in the pyramidal cell. Our study shows similar effects in NAc MS neurons mediated by K_{IR} channels, with hyperpolarization of the RMP and reduction in the amplitude and duration of EPSP in the presence of these channels. I_h channels are also found to suppress the subthreshold synaptic transmission and integration in pyramidal neurons as well as the dendritic excitability (Magee 1998). Previous studies have suggested that K_{IR} channels should modulate temporal summation and cell excitability (Wilson and Kawaguchi 1996; Uchimura *et al.* 1989a; Mermelstein *et al.* 1998). The suppression, and temporal compression, of the EPSPs in their presence has been suggested to impose a requirement for greater spatial and/or temporal coherence of excitatory inputs (Wilson and Kawaguchi 1996) to evoke firing in MS neurons (Nicola *et al.* 2004). Our results show that K_{IR} channels contribute to the modulation of cell excitability in NAc MS neurons. They were also found to participate in the normalization of amplitude of synaptic inputs at the soma, thus helping the neuron to compensate for the dendritic filtering of distal input amplitude, thereby increasing their impact on somatic V_m. Thus, dendritic K_{IR} channels are likely to be strong modulators of the propagation and integration of down-state excitatory synaptic inputs in NAc MS neurons, through effects similar to those which I_h currents exert in the pyramidal neurons of the hippocampus and neocortex (Magee 1999, 2000; Williams and Stuart 2003).

The situation is likely to be different in the up-state, however, where K_{IR} channels are largely deactivated and K_{As} channels more strongly activated. Our studies on the role of K_{As} in shaping the EPSPs in the up-state indicate that when the membrane potential is depolarized (e.g. to −65 mV), the contribution from K_{As} significantly increases. The influence of K_{As} will be exerted both on EPSPs generated during the up-state and on the spiking behaviour of the neuron. It may be noted that K_{As} has also been shown to modulate MS neuron excitability in a use-dependent manner across individual up-states (at membrane potentials more depolarized than −65 mV; Mahon *et al.* 2000b), but this effect is produced mainly by the slow inactivation of this channel, while the effects described here are attributable to the *activation* of the conductance. It may be noted that, in the up-state, the possibility cannot be ruled out that channels other than K_{IR} and K_{As} (e.g. Ca^{2+} and Na^+ channels) might also play their own, more subtle roles in regulating excitability. On the whole, it appears that while K_{IR} conductance plays a primary role in determining the electrical behaviour in the down-state and in regulating the transition from the down- to the up-state, in the up-state, K_{As} also start to play a prominent role in determining the excitability of the neuron. It is worth noting that a recent study (Mahon *et al.* 2006) has shown that this two-state membrane potential behaviour could be an artifact of anesthesia as, in the anaesthetized awake animal, the cell spends most of its time at relatively depolarized membrane potentials (~ –70 mV). Thus, in the awake animal, K_{IR} and K_{As} might act as equal determinants of the properties of incoming EPSPs and their efficiency at evoking spikes.

4.2 *Implications on MS neuron functioning*

In the neurons that express them, K_{IR} channels are believed to play an important role in a variety of cellular functions especially in regulating K^+ homeostasis, synaptic integration, neuronal firing and resting conductance (Wilson 1993; Mermelstein *et al.* 1998; Hille 2001; Perez *et al.* 2006). Our findings on the modulatory influence of K_{IR} channels on EPSPs in MS neurons indicate that neurotransmitters or modulators that are capable of varying the conductance of K_{IR} channels could affect synaptic integration and excitability in these neurons. One such example is dopamine, an important neuromodulator in striatum that is capable of

altering several voltage-dependent conductances including K_{IR} conductance, thus regulating the neuron's responsiveness to synaptic inputs (Wickens and Wilson 1998; Nicola *et al.* 2000; Gruber *et al.* 2003). Experimental studies have shown that dopamine (DA) induces hyperpolarization in NAc MS neurons by activation of D1 receptors (D1R) and depolarization through activation of D2 receptors (D2R) (Uchimura *et al.* 1986; Higashi *et al.* 1989; Uchimura and North 1990; Nicola *et al.* 2000; Perez *et al.* 2006). The dopamine-induced hyperpolarization was found to be accompanied by increase in K^+ conductance and decrease in apparent input resistance, while the depolarization was accompanied by decrease in K^+ conductance and increase in apparent input resistance (Uchimura *et al.* 1986). However, the type of K^+ conductance mediating these effects remains to be uncovered and our results help to shed light on this question. The changes in R_{in} observed in our study are both in qualitative as well as quantitative agreement with experimental data. For instance, qualitatively, hyperpolarization of the cell (induced by increase of K_{IR} conductance) was associated with a drop in R_{in}, and depolarization (induced by reduction of K_{IR} conductance) with a rise in R_{in}. For quantitative analysis we compared the DA-induced percentage changes in R_{in} at the soma observed by Uchimura *et al.* (1986) with corresponding changes of R_{in} at the soma in our model. The hyperpolarization-linked reduction of R_{in} was ~20% in the experimental study [*see* figure 1A (b) in Uchimura *et al.* (1986)], and 22.5% in our model (data not shown), while depolarization-linked enhancement of R_{in} was ~50% in the experimental study [*see* figure 1A (c) in Uchimura *et al.* (1986)], and an identical 50% in our model. As the changes in membrane potential and R_{in} in our study are elicited by alterations of K_{IR} conductance, the close quantitative agreement strongly suggests that, among the various K^+ channels present in the NAc MS neurons, K_{IR} channels are the most likely target of DA action, in agreement with the suggestion tentatively put forward by Uchimura *et al.* (1989a).

Our findings also appear to have implications for the dynamics of the networks in which NAc MS neurons are embedded. Experimental studies have shown that the excitability of MS neuron in the two regions of the NAc (core and shell) differs, shell neurons being less excitable than core neurons (O'Donnell and Grace 1993). One factor believed to contribute to this difference is the type of DA receptor (D1 and D2 receptors denoted as D1R and D2R, respectively) expressed in each region. Our results offer a plausible explanation for the observations on differential excitability. MS neurons with D1-like expressions have been correlated with the expression of substance P (SP) and are more concentrated in the shell region while neurons with D2-like receptor expression are correlated with enkephalin (ENK) expression and constitute the larger fraction in the core region (Lu *et al.* 1998; Mermelstein *et al.* 1998; Nicola *et al.* 2000). D1R-mediated inhibitory synaptic responses observed in NAc MS neurons (Pennartz *et al.* 1992) may have occurred through the reduction, and D2R-mediated excitatory responses through the augmentation of K_{IR} conductance (Perez *et al.* 2006), respectively. Taken together, our findings allow us to speculate that in shell neurons DA acting mainly through D1Rs would raise the conductance of K_{IR} channel, depressing the EPSP amplitude and half width leading to reduction in temporal summation and excitability of the neuron while in core neurons activation of D2Rs would reduce the conductance of K_{IR} channels, resulting in the enhancement of EPSP parameters and, thereby, higher excitability of the neuron.

Experimental evidence suggests that both K_{IR} and K_{As} conductances are modulated by DA concomitantly via the D1 and D2 receptors (Perez *et al.* 2006; Moyer *et al.* 2007), implying that, when DA acts on the accumbal MS neuron, both conductances might participate in mediating its effects. However, the ranges of membrane potential at which these conductances operate are different. This is because, as discussed above, K_{IR} dominates in the down-state, influencing the transitions to the up-state, while effects of K_{As} on EPSPs and spiking are exerted in the up-state. Previous work in this area suggests that the K_{As} conductance is not modulated through D1 receptors while activation of D2 receptors produces an increase in this conductance of up to 10% (Moyer *et al.* 2007). Since in our simulations increase in K_{As} conductance decreases the cell excitability, our findings suggest that DA acting on K_{As} via D2 would reduce the excitability of the MS neuron during the up-state. Such an effect has in fact been observed experimentally in an earlier work, where the application of D2R agonists was shown to suppress the up-state spiking frequency in rat accumbal neurons (Perez *et al.* 2006).

Since K_{IR} and K_{As} are powerful modulators of EPSP properties, it is conceivable that sets of MS neurons expressing different densities of K_{IR} and K_{As} conductances would display appreciably different excitabilities. As of now, there seems to be no information on variation of K_{IR} or K_{As} density among different accumbal MS neurons. However, there exist two distinct regions of the NAc, the core and the shell, whose MS neurons show differences in the levels of inactivation expressed in the K_{IR} conductance, and these differences have been shown to result in different excitabilities (Mermelstein *et al.* 1998; Steephen and Manchanda 2009). This indicates that if differences in density of channel conductances, or in other important biophysical parameters, were to be expressed in distinct subsets of neurons within the NAc, separate accumbal input processing streams could arise that exhibit different excitabilities.

The question remains as to whether background noise present in electrophysiological recordings in MS neurons might mask the findings that we have reported when these are elicited experimentally. However, considering the magnitude of the changes observed in our study, it is probable that these changes will also be observed in experimental situations designed to test these ideas. For example, the percentage effects observed upon raising or diminishing the K_{IR} conductance on the salient parameters studies here (e.g. EPSP amplitude and time course, half attenuation distance, membrane time constant and input resistance) are appreciable, and should be readily observable in experimental recordings, at least in those cases where noise is not a major contaminant of the signals. As an example, the amplitude of the EPSP increased by between 25% and 60% when the conductance of K_{IR} was varied to different degrees. The level of noise observed in experimental recordings from NAc MS neurons (O'Donnell and Grace 1995, 1998; O'Donnell *et al*. 1999; O'Donnell 2003) is ~1–2 mV, which would conceivably confound the observation of effects in the case of signals of very low amplitude, but not of relatively high amplitude signals. However, in experimental studies, steps are usually taken to enhance the discrimination of signal from noise, for example, statistical analysis of effects over several trials, as well as signal conditioning and processing techniques that improve signal to noise ratio, strategies that can accentuate changes subtler than those observed in the present work.

5. Conclusion

Our study demonstrates that, in NAc Ms neurons, reduction in K_{IR} and K_{As} conductances results in a facilitatory influence, whereas their enhancement produces an inhibitory influence on EPSPs in the down-state and depolarized up-state, respectively, of the neuron. These effects should modulate synaptic integration in these neurons, which in turn, modulate their spiking behaviour, as verified in our study. The predictions made by this study are experimentally testable because our conclusions are based mainly on somatic data; and electrophysiological recordings, although technically challenging, are carried out by several groups from the somata of NAc MS neurons (Uchimura *et al*. 1989b; O'Donnell and Grace 1993; Perez *et al*. 2006). The strength of the predictions made by computational models of neurons depends strongly on the fidelity of the model with respect to the actual neuron. The results of the validation of responses from our model (see the methods section), built using knowledge currently available about NAc MS neurons from the experimental literature, place confidence in the reliability of our predictions. However, the accuracy of the model as well as the robustness of these predictions may be enhanced by improvements in the model resulting from superior characterization of the channel parameters and their densities and distribution. For example, in our model, the value of $[Ca^{2+}]_i$ at rest is high (1 mM) when compared with the experimental literature available for the resting $[Ca^{2+}]_i$ in other neurons (~0.2–0.3 mM). This value was obtained from the original model by Wolf *et al.* (2005), which they adopted to match the experimental results from MS neurons. The value of $[Ca^{2+}]_i$ in the model remains subject to revision in light of pertinent experimental evidence. Also, the fraction of receptor currents mediated by the individual ions may be calculated separately when data for the conductances of receptor channels for each of these ions is known differentially. This would yield an improvement over the approximation we adopted in our model, of estimating a fixed fraction of receptor currents as Ca^{2+} currents. Further improvements would result from using a model with real morphology instead of a stylized one.

Acknowledgements

The authors would like to thank the Department of Biotechnology, New Delhi, for their financial support for this work (project no. BT/PR9599/Med/30/34/2007).

References

Biel M, Wahl-Schott C, Michalakis S and Zong X 2009 Hyperpolarization-activated cation channels: from genes to function. *Physiol. Rev*. **89** 847–885

Brady AM and O'Donnell P 2004 Dopaminergic modulation of prefrontal cortical input to nucleus accumbens neurons *in vivo*. *J. Neurosci*. **24** 1040–1049

Carelli RM 2004 Nucleus accumbens cell firing and rapid dopamine signaling during goal-directed behaviors in rats. *Neuropharmacology* **47** 180–189

Carlezon WA and Thomas MJ 2009 Biological substrates of reward and aversion: A nucleus accumbens activity hypothesis. *Neuropharmacology* **56** 122–132

Carnevale T and Hines M 2006 *The NEURON book* (Cambridge: Cambridge University Press)

Carter AG, Soler-Llavina GJ and Sabatini BL 2007 Timing and location of synaptic inputs determine modes of subthreshold integration in striatal medium spiny neurons. *J. Neurosci*. **27** 8967–8977

Cooper DC 2002 The significance of action potential bursting in the brain reward circuit. *Neurochem. Int*. **41** 333–340

Cooper DC and White FJ 2000 L-type calcium channels modulate glutamate-driven bursting activity in the nucleus accumbens *in vivo*. *Brain Res.* **880** 212–218

French SJ and Totterdell S 2002 Hippocampal and prefrontal cortical inputs monosynaptically converge with individual projection neurons of the nucleus accumbens. *J. Comp. Neurol*. **446** 151–165

French SJ and Totterdell S 2003 Individual nucleus accumbens-projection neurons receive both basolateral amygdala and ventral subicular afferents in rats. *Neuroscience* **119** 19–31

Goto Y and Grace AA 2005a Dopamine-dependent interactions between limbic and prefrontal cortical plasticity in the nucleus accumbens: disruption by cocaine sensitization. *Neuron* **47** 255–266

Goto Y and Grace AA 2005b Dopaminergic modulation of limbic and cortical drive of nucleus accumbens in goal-directed behavior. *Nat. Neurosci.* **8** 805–812

Goto Y and Grace AA 2008 Limbic and cortical information processing in the nucleus accumbens. *Trends Neurosci*. **31** 552–558

Goto Y and O'Donnell P 2002 Timing-dependent limbic-motor synaptic integration in the nucleus accumbens. *Proc. Natl. Acad. Sci. USA* **99** 13189–13193

Grace AA 2000 Gating of information flow within the limbic system and the pathophysiology of schizophrenia. *Brain Res. Rev*. **31** 330–341

Gruber AJ, Solla SA, Surmeier DJ and Houk JC 2003 Modulation of striatal single units by expected reward: a spiny neuron model displaying dopamine-induced bistability. *J. Neurophysiol.* **90** 1095–1114

Higashi H, Inanaka K, Nishi S and Uchimura N 1989 Enhancement of dopamine actions on rat nucleus accumbens neurones *in vitro* after methamphetamine pre-treatment. *J. Physiol. (London)* **408** 587–603

Hille H 2001 *Ion channels of excitable membranes* (Massachussetts: Sinauer Associates) pp. 25–60

John J and Manchanda R 2009 K_{IR} channels in nucleus accumbens MS neurons modulate integration of excitatory synaptic inputs: A computational study. *BMC Neuroscience (Suppl 1)* **10** 33

Johnston D, Magee JC, Colbert CM and Christie BR 1996 Active properties of neuronal dendrites. *Annu. Rev. Neurosci*. **19** 165–186

Johnston D and Wu SM 1995 *Foundations of cellular neurophysiology* 1st edition (Cambridge: MIT Press) p 192

Kalivas PW and Nakamura M 1999 Neural systems for behavioral activation and reward. *Curr. Opin. Neurobiol*. **9** 223–227

Koch C, Rapp M and Segev I 1996 A brief history of time (constants). *Cereb. Cortex* **6** 93–101

Kubo Y, Baldwin TJ, Jan YN and Jan LY 1993 Primary structure and functional expression of a mouse inward rectifier potassium channel. *Nature (London)* **362** 127–133

Lu XY, Ghasemzadeh MB and Kalivas PW 1998 Expression of D1 receptor, D2 receptor, substance P and enkephalin messenger RNAs in the neurons projecting from the nucleus accumbens. *Neuroscience* **82** 767–780

Magee JC 1998 Dendritic hyperpolarization-activated currents modify the integrative properties of hippocampal CA1 pyramidal neurons. *J. Neurosci*. **18** 7613–7624

Magee JC 1999 Dendritic Ih normalizes temporal summation in hippocampal CA1 neurons. *Nat. Neurosci*. **2** 508–514

Magee JC 2000 Dendritic integration of excitatory synaptic input, *Nat. Neurosci*. **1** 181–190

Magee JC and Cook EP 2000 Somatic EPSP amplitude is independent of synapse location in hippocampal pyramidal neurons. *Nat. Neurosci.* **3** 895–903

Magee J, Hoffman D, Colbert C and Johnston D 1998 Electrical and calcium signaling in dendrites of hippocampal pyramidal neurons. *Annu. Rev. Physiol*. **60** 327–346

Mahon S, Vautrelle N, Pezard L, Slaght SJ, Deniau JM, Chouvet G and Chrpier S 2006 Distinct patterns of striatal medium spiny neuron activity during the natural sleep-wake cycle. *J. Neurosci.* **26** 12587–12595

Mahon S, Deniau JM, Charpier S and Delord B 2000a Role of a striatal slowly inactivating potassium current in short-term facilitation of corticostriatal inputs: a computer simulation study. *Learn Mem.* **7** 357–362

Mahon S, Delord B, Deniau JM and Charpier S 2000b Intrinsic properties of rat striatal output neurones and time-dependent facilitation of cortical inputs *in vivo*. *J. Physiol.* **527** 345–354

McGinty VB and Grace AA 2009 Timing-dependent regulation of evoked spiking in nucleus accumbens neurons by integration of limbic and prefrontal cortical inputs. *J. Neurophysiol*. **101** 1823–1835

Meredith GE, Agolia R, Arts MPM, Groenewegen HJ and Zahm DS 1992 Morphological differences between projection neurons of the core and shell in the nucleus accumbens of the rat. *Neuroscience* **50** 149–162

Meredith GE, Baldo BA, Andrejewski ME and Kelly AE 2008 The structural basis for mapping behavior onto the ventral striatum and its subdivisions. *Brain Struct. Funct.* **213** 17–27

Meredith GE and Totterdell S 1999 Microcircuits in nucleus accumbens' shell and core involved in cognition and reward. *Psychobiology* **27** 165–186

Mermelstein PG, Song WJ, Tkatch T, Yan Z and Surmeier DJ 1998 Inwardly rectifying potassium (irk) currents are correlated with IRK subunit expression in rat nucleus accumbens medium spiny neurons. *J. Neurosci*. **18** 6650–6661

Migliore M and Shepherd GM 2002 Emerging rules for the distributions of active dendritic conductances. *Nat. Rev. Neurosci*. **3** 362–370

Mogenson GJ 1987 Limbic-motor integration. *Prog. Psychobiol. Physiol. Psychol*. **12** 117–170

Mogenson GJ, Jones DL and Yim CY 1980 From motivation into action: functional interface between the limbic system and motor system. *Prog. Neurobiol*. **14** 69–97

Moyer JT, Wolf JA and Finkel LH 2007 Effects of dopaminergic modulation on the integrative properties of the ventral striatal medium spiny neuron. *J. Neurophysiol*. **98** 3731–3748

Nicola SM, Hopf FW and Hjelmstad GO 2004 Contrast enhancement: a physiological effect of striatal dopamine? *Cell Tissue Res*. **318** 93–106

Nicola SM, Surmeier DJ and Malenka RC 2000 Dopaminergic modulation of neuronal excitability in the striatum and nucleus accumbens. *Annu. Rev. Neurosci*. **23** 185–215

Nisenbaum ES and Wilson CJ 1995 Potassium currents responsible for inward and outward rectification in rat neostriatal spiny projection neurons. *J. Neurosci.* **15** 4449–4463

Nisenbaum ES, Xu ZC and Wilson CJ 1994 Contribution of a slowly inactivating potassium current to the transition to firing of neostriatal spiny projection neurons. *J. Neurophysiol.* **71** 1174–1189

North RA and Uchimura N 1989 5-hydroxytryptamine acts at 5-HT_2 receptors to decrease potassium conductance in rat nucleus accumbens neurons. *J. Physiol. (London)* **417** 1–12

O'Donnell P, Greene J, Pabello N, Lewis BL and Grace AA 1999 Modulation of cell firing in the nucleus accumbens. *Ann. N.Y. Acad. Sci.* **877** 157–175

O'Donnell P 2003 Dopamine gating of forebrain neural ensembles. *Eur. J. Neurosci.* **17** 429–435

O'Donnell P and Grace AA 1993 Physiological and morphological properties of accumbens core and shell neurons recorded *in vitro*. *Synapse* **13** 135–160

O'Donnell P and Grace AA 1995 Synaptic interactions among excitatory afferents to nucleus accumbens neurons: hippocampal gating of prefrontal cortical input. *J. Neurosci.* **15** 3622–3639

O'Donnell P and Grace AA 1998 Dysfunctions in multiple interrelated systems as the neurobiological bases of schizophrenic symptom clusters. *Schizophr. Bull.* **24** 267–283

Pawlak V and Kerr JND 2008 Dopamine receptor activation is required for corticostriatal spike-timing-dependent plasticity. *J. Neurosci*. **28** 2345–2446

Pennartz CMA, Dolleman-Van der Weel MJ and Lopes da Silva FH 1992 Differential membrane properties and dopamine effects in the shell and core of the rat nucleus accumbens studied *in vitro*. *Neurosci. Lett*. **136** 109–112

Perez MF, White FJ and Hu X 2006 Dopamine D2 receptor modulation of K^+ channel activity regulates excitability of nucleus accumbens neurons at different membrane potentials. *J. Neurophysiol*. **96** 2217–2228

Reyes A 2001 Influence of dendritic conductances on input-output properties of neurons. *Annu. Rev. Neurosci*. **24** 653–675

Reynolds JNJ, Hyland BI and Wickens JR 2001 A cellular mechanism of reward-related learning. *Nature (London)* **413** 67–70

Samuelsson E and Kotaleski JH 2007 Exploring GABAergic and dopaminergic effects in a minimal model of a medium spiny projection neuron. *Neurocomputing* **70** 1651–1618

Schultz W 1998 Predictive reward signal of dopamine neurons. *J. Neurophysiol*. **80** 1–27

Schultz W, Trembley L and Hollerman JR 2003 Changes in behavior related neuronal activity in the striatum during learning. *Trends Neurosci*. **26** 321–328

Smith AD and Bolam JP 1990 The neural network of the basal ganglia as revealed by the study of synaptic connections of identified neurons. *Trends Neurosci.* **13** 259–265

Steephen JE and Manchanda R 2009 Differences in biophysical properties of nucleus accumbens medium spiny neurons emerging from inactivation of inward rectifying potassium currents. *J. Comput. Neurosci*. **27** 453–470

Taverna S, van Dongen YC, Groenewegen HJ and Pennartz CM 2004 Direct physiological evidence for synaptic connectivity between medium-sized spiny neurons in rat nucleus accumbens *in situ. J. Neurophysiol.* **91** 1111–1121

Uchimura N, Higashi H and Nishi S 1986 Hyperpolarizing and depolarizing actions of dopamine via D-1 and D-2 receptors on nucleus accumbens neurons. *Brain Res*. **375** 368–372

Uchimura N, Cherubini E and North RA 1989a Inward rectification in rat nucleus accumbens neurons. *J. Neurophysiol*. **62** 1280–1286

Uchimura N, Higashi H and Nishi S 1989b Membrane properties and synaptic responses of the guinea pig nucleus accumbens neurons *in vitro*. *J. Neurophysiol*. **61** 769–779

Uchimura N and North RA 1990 Actions of cocaine on rat nucleus accumbens neurones *in vitro*. *Br. J. Pharmacol*. **99** 736–740

Wickens JR and Wilson CJ 1998 Regulation of action-potential firing in spiny neurons of the rat neostriatum *in vivo. J. Neurophysiol*. **79** 2358–2364

Williams SR and Stuart GJ 2000 Site independence of EPSP time course is mediated by dendritic I_h in neocortical pyramidal neurons. *J. Neurophysiol*. **83** 3177–3182

Williams SR and Stuart GJ 2003 Role of dendritic synapse location in the control of action potential output. *Trends Neurosci*. **26** 147–154

Wilson CJ 1992 Dendritic morphology, inward rectification, and the functional properties of neostriatal neurons; in *Single neuron computation* (eds) T McKenna, J Davis and S Zornetzer (Academic Press Inc.) pp. 141–171

Wilson CJ 1993 The generation of natural firing patterns in neostriatal neurons. *Prog. Brain Res*. **99** 2397–2410

Wilson CJ 1995 Dynamic modification of dendritic cable properties and synaptic transmission by voltage-gated potassium channels. *J. Comput. Neurosci*. **2** 91–115

Wilson CJ and Kawaguchi Y 1996 The origins of two-state spontaneous membrane potential fluctuations of neostriatal spiny neurons. *J. Neurosci.* **16** 2397–2410

Wolf JA, Schroeder LF and Finkel LH 2001 Computational modeling of medium spiny projection neurons in nucleus accumbens: toward the cellular mechanisms of afferent stream integration. *Proc. IEEE* **89** 1083 –1092

Wolf JA, Moyer JT, Lazarewicz MT, Contreras D, Benoit-Marand M, O'Donnel P and Finkel LH 2005 NMDA/AMPA ratio impacts state transitions and entrainment to oscillations in a computational model of the nucleus accumbens medium spiny projection neuron. *J. Neurosci*. **25** 9080–9095

Wolf ME 2002 Addiction: making the connection between behavioral changes and neuronal plasticity in specific pathways. *Mol. Interv*. **3** 147–157

Yang CR and Mogenson GJ 1984 Dopamine enhances terminal excitability of hippocampal-accumbens neurons via D2 receptor: role of dopamine in presynaptic inhibition. *J. Neurosci*. **6** 2470–2478

MS received 24 May 2010; accepted 04 February 2011

*e*Publication: 16 May 2011

Corresponding editor: Neeraj Jain